Negatively Charged Conical Electrostatic Probes in a Supersonic Flow

W. E. SCHARFMAN*
Stanford Research Institute, Menlo Park, Calif.
AND
A. G. HAMMITT†
TRW Systems Group, Redondo Beach, Calif.

An experimental investigation of the current drawn by a negatively biased conical probe in a supersonic air plasma stream has been accomplished using a shock tube. The experimental results are in fair agreement with the theoretical analyses which have been performed and provide a means of relating the readings of such a probe to the plasma ion density.

Nomenclature

a = width of waveguide (interferometer)
e = electron charge
I = current to probe
J = dimensionless probe current $I/\pi e u_\infty n_i L^2 \sin\theta$
K = ion mobility
Kn = Knudsen number based on probe length
L = path length between horns (microwave interferometer) or probe length
M = Mach number
m = particle mass
n = particle density
Re_L = Reynolds number based on probe length
S = dimensionless mobility
Sc_i = ion Schmidt number
T/T_w = fluid to probe temperature ratio
u_∞ = freestream velocity
α = angle of attack
$\Delta\Phi$ = phase difference in radians (microwave interferometer)
ε_o = dielectric constant
θ = conical probe half-angle
λ_D/L = Debye length over probe length
λ_o = free space wavelength (microwave interferometer)
λ_ϕ/L = $(\lambda_D/L)(\phi_T)^{1/2}$
ϕ_p = probe potential
ϕ_T = electric potential to thermal energy ratio $(e\phi_p/kT)$
ω = frequency (microwave interferometer)
ω_p = plasma radian frequency $(n_e e^2/m_e \varepsilon_o)^2$ (microwave interferometer)

Subscripts
i = ion
e = electron

1. Introduction

CONICAL electrostatic probes biased negatively have been flown on the RMP-B program to measure charge density in the wake. The probes are mounted on a sphere which is injected into the wake. At the start of this study the understanding of the operation of such probes was inadequate for interpreting the measured current in terms of charge density. To improve this understanding, an experimental and theoretical program was jointly undertaken by the Stanford Research Institute (SRI) and TRW Systems Group with SRI performing the experimental part and TRW the theoretical part of the program.

The range of experimental parameters was chosen so that it encompassed the expected flight regime and also allowed the scaling features of the theory to be checked.

The theoretical analysis showed that the most important parameter affecting probe current was a dimensionless mobility S defined as[1]

$$S = 1/Re_L Sc_i(\lambda_D/L)^2 \tag{1}$$

The experiments were designed to vary S over approximately 5 orders of magnitude.

2. Experimental Program

In order to check various theoretical aspects of conical electrostatic probes, an experimental program was carried out in the SRI 12-in.-diam arc-heated, pressure-driven shock tube. Because of the large diameter of the tube it was possible to mount six different conical probes and thus obtain six pieces of information on each shot. The six probes were designed so that the effect of probe length and probe voltage could be studied. Thus, three different cone lengths were chosen; all of these probes to be run at the same bias voltage. The other three probes were of the same length but had different applied voltages. The probe lengths and voltages are listed in Table 1.

Table 1 Probe characteristics

Probe length, cm	Probe voltage, v
0.11	−9
1.1	−9
5.3	−9
1.1	−3
1.1	−30
1.1	−90

The probe length varied by a factor of 50 while the probe voltage varied by a factor of 30. All voltages were negative so that the collected current was limited by ion flow. The other electrode was the shock tube walls and probe mounting structure. Midway through the tests the dielectric supports holding the conical electrodes were silver painted to minimize transient effects. This silver paint also acted as part of the return electrode system. The cones all had 15° half-angles, with a nose bluntness of less than 0.1 of the base radius. Figure 1 is a drawing of the three probes used.

Three initial shock tube pressures were used and three different charge densities at each pressure, so that a total of nine flow conditions were used. The nominal values are shown in Table 2.

Presented as Paper 71-143 at the AIAA 9th Aerospace Sciences Meeting, New York, January 25–27, 1971; submitted February 24, 1971, revision received September 27, 1971. This research was supported by the Bell Telephone Laboratory.

* Program Manager, Electromagnetic Sciences Laboratory.
† Senior Staff Engineer, Research and Technology Operations. Member AIAA.

Table 2 Initial shock tube pressures and charge

Initial pressure, torr	Charge density, el/cm^3
0.03	1×10^9
0.3	5.6×10^9
3.0	5×10^{10}
0.03	1.1×10^{10}
0.3	1.3×10^{11}
3.0	1×10^{12}
0.03	2.8×10^{11}
0.3	2.5×10^{12}
3.0	2.3×10^{13}

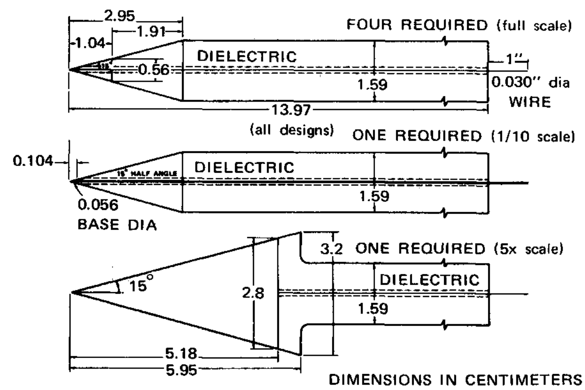

Fig. 1 Conical probe electrode configurations.

This range of pressure and charge density encompassed the expected flight values of S. The freestream conditions were determined by several sensors. Flush ion probes and pressure probes were used to detect the shock front passage down the tube to yield shock velocity. From this quantity the equilibrium pressure, gas temperature and charge density were found.

Since equilibrium charge density was not always achieved, especially at the lowest pressure, the charge density was also measured using 0.01×0.50 in. cylindrical probes perpendicular to the flow and a specially constructed microwave interferometer.

It was observed with an interferometer using small horn antennas in the metal shock tube, phase shifts as large as those produced by a plasma of 10^{10} electrons/cm^3 could be produced by a metal rod inserted in the tube 10 ft upstream of the interferometer. This was evidence of electromagnetic energy being coupled from the interferometer to the shock tube with sufficient strength to prevent measurement at a value of $n_e \leqq 10^{10}$ electrons/cm^3. Shots at these values showed large variation in phase even before the shock reached the interferometer antennas.

To decrease this coupling, an aerodynamically transparent waveguide was designed that would guide most of the electromagnetic (EM) energy but allow the shocked gas to pass through it without a change in plasma density.[3] Essentially the waveguide consisted of the top and bottom plates of a section of rectangular waveguide machined to a wedge shape to minimize flow disturbances in the guide. The side walls were removed to allow the gas to flow through, but the EM energy was kept in the guide by free molecular (2-mil-diam) wires that were spaced closely enough (3/8 in.) to prevent significant EM energy leakage.

This section was checked by measuring the phase shift of a section of polyfoam inserted into a piece of standard waveguide. The results checked to better than 10%.

The expression for the change of phase in the waveguide section can be found from Jordan[2] by substituting in the dielectric constant of the plasma. The result is[3]

$$\Delta\Phi = \frac{2\pi L}{\lambda_o}\left[1-\left(\frac{\lambda_o}{2a}\right)^2\right]^{1/2}\left\{1-\left[1-\frac{(\omega_p/\omega)^2}{1-(\lambda_o/2a)^2}\right]^{1/2}\right\} \quad (2)$$

3. Experimental Results

The cylindrical probes had previously been checked against a microwave interferometer and were shown to agree with the microwave inferred density at pressures less than 0.1 torr.[3] An initial shock tube pressure of 1.0 torr gave erroneous results for charge densities greater than about 3×10^{10} electrons/cm^3. Therefore their use at 0.3 torr is uncertain. The present results showed that at 0.3 torr the cylindrical probe agreed quite well with the microwave interferometer over the entire range of charge densities where comparisons were possible. At charge densities where the microwaves were cut off, the cylindrical probe checked the equilibrium values quite closely.

At an initial pressure of 0.03 torr, similar good agreement between probe and interferometer was found. The probe generally indicated slightly higher charge densities than the interferometer. This may be attributed to boundary-layer effects on the interferometer waveguide section. The derivation of phase change as a function of charge density shown earlier is for a uniform rectangular slab of plasma, whereas in the actual case, boundary layer growth along the waveguide walls will reduce the charge density near the walls. This will reduce the phase shift somewhat from the uniform slab model or if the slab model is used to infer charge density, it will lead to low values of charge density. It is estimated that at the lowest pressure (0.03 torr) the boundary-layer effect may lead to charge densities too low by about 30%. At 3.0 torr, equilibrium values were used for the charge density. Wedge-shaped probes were also used and indicated densities in good agreement with the equilibrium values when interpreted using theory discussed in Ref. 4.

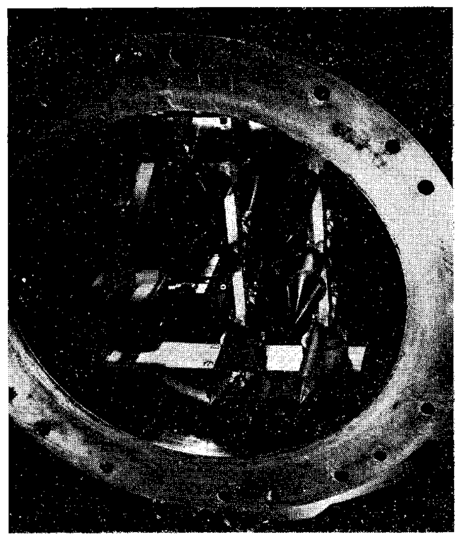

Fig. 2 Photograph of the conical probes and interferometer mounted in the shock tube.

A photograph of the probes mounted in the shock tube along with the interferometer is shown in Fig. 2. The bars holding the probes were adjustable in angle so that each rack of three probes could be set at an angle of attack.

A typical set of data are shown in Fig. 3. The current as a function of time for the six conical probes is shown, as well as the cylindrical probe current and the interferometer output.

Data were read at a time behind the shock front at which the current was relatively steady and was the same for each probe. This time changed from shot to shot. Allowance was made for the fact that it took approximately 20 μsec for the flow to cover the largest probe. Data were never taken at times shorter than one flow time (probe length velocity). The interferometer was mounted a few centimeters downstream of the conical probe electrodes while the cylindrical wire probe was mounted a few cm upstream. Therefore, the probe responses shown in Fig. 3 show the wire probe indicating current at earlier times than the conical probes, while the interferometer indicated plasma at somewhat later times. The data were read from each sensor at a fixed time after the arrival of the plasma front at the sensor. These times are indicated in Fig. 3.

The estimated accuracy of the freestream charge density is less than a factor of two. Agreement between the different methods of determining charge density were generally of that order.

Data from every shot were read although when a new flow condition was being measured the scope sensitivities might have been set so that only small deflections were recorded.

On some shots a steady test slug may have never been established. In order to discriminate between the quality of the data in the comparison with the theoretical models, the data were sorted into grades A, B, C (A being judged the best and C the worst). Data were judged of A quality if all sensors showed similar current-time records, had a relatively stable uniform current region, and had sufficient deflection to be read with good accuracy. B and C quality data had failings in these standards.

At an applied voltage of -90 v, voltage breakdown of the conical probe occurred for a number of the flow conditions. This was seen either by sporadic large increases of current (as in Fig. 3) or a general current level orders of magnitude larger than the probes with lower bias.

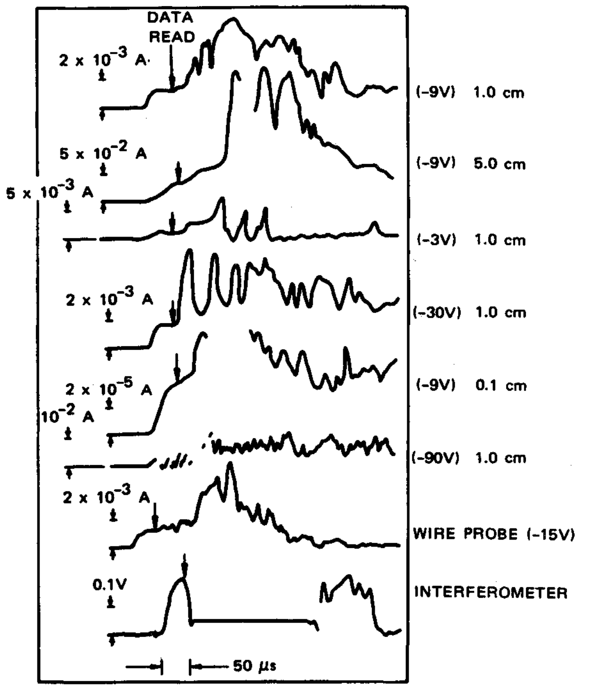

Fig. 3 Set of data showing probe currents and interferometer output as a function of time.

4. Data Evaluation

Governing Parameters

The data from the various shock-tube shots have been reduced to show the pertinent parameters. Various dimensionless quantities such as those given in Table 3 should be considered.

Table 3 Governing parameters

Input parameters		
Neutral-fluid parameters	Charged-particle parameters	Output parameter
Reynolds number, Re_L 25–1(10⁵)	Debye length, λ_D/L 0.1–0.2(10^{-5})	Electric-current to convective-charge-flux ratio, J 0.01–1
Knudsen number, Kn 0.15–0.3(10^{-5})	Electron-potential to thermal-energy ratio, ϕ_T −7– −360	
Fluid-to-probe temperature ratio, T/T_w 9–12	Dimensionless mobility, S 2–10^5	
	Ion Schmidt number, Sc_i	
Mach number, M 2.5–3.0	Based on conditions ahead of probe 0.35	

The tests which were run covered a range in all these parameters except Schmidt number and Mach number (proportional to Re times Kn) and the fluid to probe temperature ratio. These quantities only changed by small amounts because of the restrictions imposed by the nature of the shock tube tests. The Mach number relative to the probe is in the range of 2.5–3.0 for all shots, the fluid to probe temperature ratio is between 9 and 12, and the ion Schmidt number about 0.35. The probes are essentially at room temperature during the entire process. The other parameters ranged over several orders of magnitude as given previously.

Not all of the dimensionless parameters tested are independent. Because of the consistency of the Mach number, the Reynolds number and Knudsen number cannot be considered independent parameters.

Since

$$S = 1/Re_L Sc_i (\lambda_D/L)^2 \tag{3}$$

one of these parameters is not independent. Since Sc_i, M, and T/T_w are constant, they cannot be considered parameters of the experiment. A complete set of dimensionless input parameters would be three of the parameters listed, selected so that they are independent. The parameters which will be used in succeeding data presentation and discussion are ϕ_T, S and Kn, or λ_D/L as convenient. ($\lambda_\phi/L = \lambda_D/L(\phi_T)^{1/2}$ may also be used in place of λ_D/L for various reasons which will be explained.) The advantage of using Kn for presenting the data from these experiments is that it was held constant over a group of shots and then varied by definite steps. λ_D/L varies continuously from shot to shot. It should be kept in mind that for ϕ_T and S constant, a change in Kn implies a change in λ_D/L. ϕ_T also varies in definite steps with the probe bias potential, while S varies continuously and is a good parameter against which to plot the data.

Considerations Based on Theoretical Analysis

The theoretical analyses which seem appropriate for describing the conditions in these experiments are those of Hammitt,[1] Denison,[5] DeBoer and Johnson,[6] Dukowicz,[7] and Baum and Denison.[8] Because of the large values of electric potential used on these probes, Denison's[5] solution is only appropriate to the present experiments as an asymptotic limit for large values of S. The effects of the neutral fluid flow parameters over the range of interest for these experiments are only considered by Baum and Denison.[8] However, these calculations indicate that the variation of the neutral fluid parameters do not have a major effect. Hammitt[1] and DeBoer and Johnson[6] both consider a uniform flow of neutral fluid, while Dukowicz[7] considers the case of a neutral incompressible flow about a cone.

The analyses[1,5,8] show that if the sheath is thin, with respect to the probe radius, the number of parameters can be reduced by one. Two charged particle fluid parameters, S and ϕ_T, are of principal importance. The Debye length can be eliminated as an independent parameter by properly combining it with the probe current parameter. Asymptotic limits exist both for ϕ_T large or small. For $\phi_T \ll 1$, the solution results in a probe current parameter, $J/(\lambda_D/L)$,[1] involving λ_D and for $\phi_T \gg 1$, the resulting probe current parameters, $J/(\lambda_\phi/L)$, Ref. 6, involves $\lambda_\phi = \lambda_D(\phi_T)^{1/2}$. For intermediate values, ϕ_T is a parameter and either probe current parameter is useful. The most suitable probe current parameter is the one which shows the least variation with ϕ_T, and this choice depends upon whether ϕ_T is large or small. Since $\phi_T \gg 1$ for these experimental results, the parameters suitable for the asymptotic limit of $\phi_T \gg 1$, $J/(\lambda_\phi/L)$, will be used to correlate the experiments. For constant bias voltage, these two parameters are essentially the same. Using these parameters, λ_D, and consequently Kn, should not appear as important additional parameters over the range in which these theoretical results are applicable.

The theories are based on the assumption that the fluid may be treated as a continuum and that the boundary layers are thin. This assumption requires a small Knudsen number. The theories also require that the sheath be thin with respect to the probe radius, which implies λ_ϕ/L small. Both of these limits restrict the range of Kn or λ_ϕ/L in which the data should be independent of Kn and λ_ϕ/L, if S, $J/(\lambda_\phi/L)$, and ϕ_T are the parameters used to correlate the data.

Results

A summary of the test conditions is given in Tables 1 and 2. The individual probe size and bias voltage are given in Table 1, and the shock tube conditions in Table 2.

The calculation of S requires a value of the mobility of NO^+ ions in air. The values given in Ref. 9 have been used. The choice of the correct value of this ion mobility is probably the most uncertain of the important properties of the gas which must be used in the data reduction process and directly affects the comparison with theory.

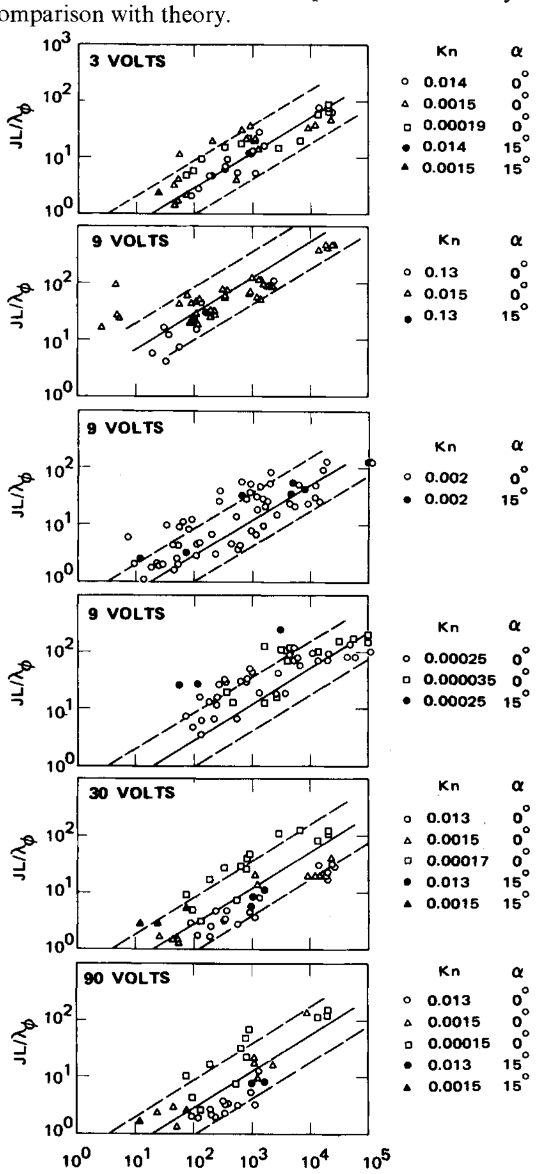

Fig. 4 Dimensionless probe current JL/λ_ϕ vs probe length mobility parameter S.

The data have been presented in Figs. 4 and 5. In Fig. 5, the nondimensional current parameter J is used, which is simply the probe current divided by probe area and freestream ion flux. In Fig. 4, the current parameter $J/(\lambda_\phi/L)$ has been used. Different symbols are used to differentiate between data at different Knudsen numbers. The Knudsen numbers tend to fall into distinct groups, while the Debye lengths are fairly uniformly spread, so it is more convenient to designate the points by Kn. For the values of M and Sc_i for which the experiments were run, the value of λ_ϕ/L can be obtained from Kn and S by the relation

$$\lambda_\phi/L = 1.2(Kn\phi_T/S)^{1/2} \tag{4}$$

All the -3, -30, and -90 v bias results have been presented on single figures. All the results at each of these bias voltages come from the same probe on successive shots. However, the -9 v bias data are from three different probes of different sizes. More data are available at this potential, which has been divided into three separate figures in order to provide clarity.

An average line through the data has been shown in Fig. 5 and also parallel lines, a factor of 3, on each side of the average line. These lines bracket most of the data and on the log plot have a slope of 2/3.

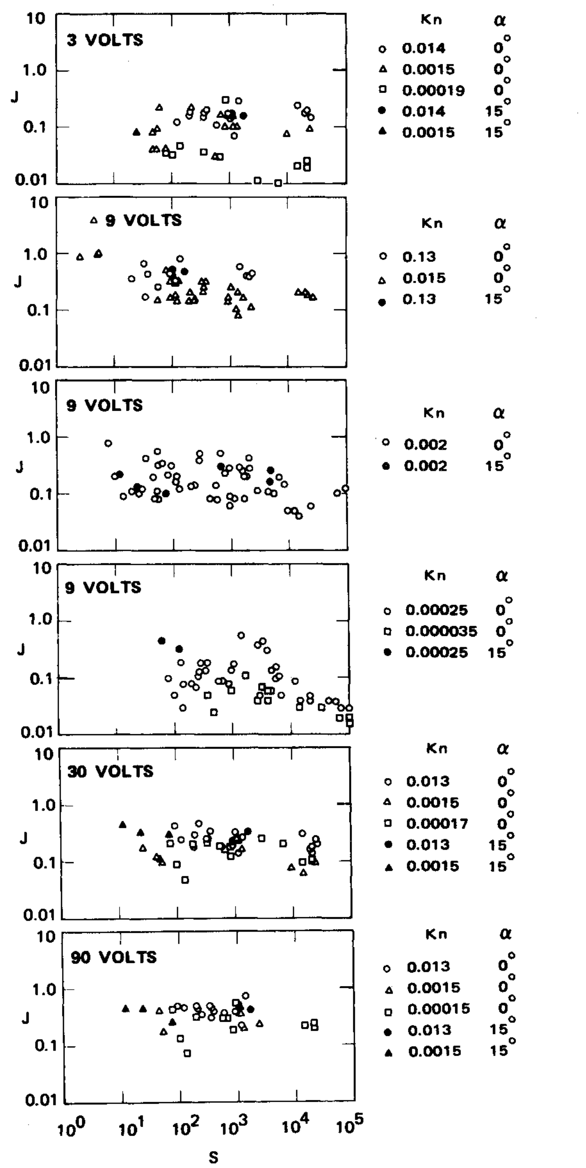

Fig. 5 Dimensionless probe current flux vs probe length mobility parameter S.

Data for probes both at zero angle of attack and at a 15° angle of attack are shown on these figures. The 15° angle-of-attack results do not appear to be noticeably different from the zero degree angle of attack, showing that angles of attack up to 15° have little effect. The one exception occurs in Fig. 5 where the angle of attack results are clearly above the zero angle of attack data.

The data have been presented on these two different plots, Figs. 4 and 5, in order to assess the value of the current parameter $J/(\lambda_\phi/L)$ suggested by the theories as compared with the simpler parameter of J. Dimensional arguments show that either plot is adequate to correlate the data; however, theory[1,5,6,8] suggests that if the parameter $J/(\lambda_\phi/L)$ is used, then over a reasonable range of Kn or λ_ϕ/L, the effect of Kn will be small, and that the effect of ϕ_T will be reduced. A comparison of the two figures does not really show this reduction of the effect of Kn. The scatter of the data is such that the effect of Kn on either plot is obscured. At a given value of S, the maximum range of Kn is about 100, so the λ_ϕ/L range is about 10, which lies within the bands of a factor of 3 in either direction.

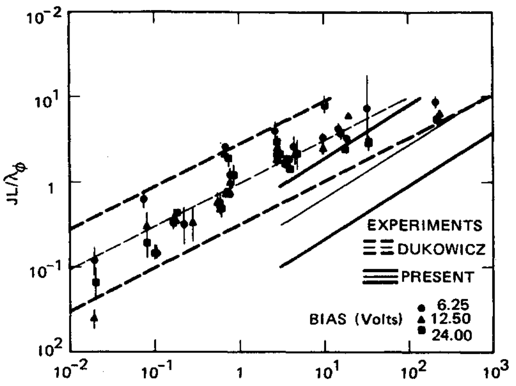

Fig. 6 Comparison of experimental results.

A similar set of experimental data have been reported by Dukowicz.[7] In Fig. 6, these data have been presented on the sample type of plot as Fig. 5. The range of the parameters lies at somewhat lower S values than the present experiments, but there is a substantial region of overlap. The spread of the data appears to be about the same as the present data and to be in reasonable agreement with the present data. The line drawn as an average of the data in Fig. 5 is also shown in this figure. The data of Ref. 7 lie above that from the extrapolation of the work. A similar set of lines has been drawn through these data. These lines may have a smaller slope equal to $\frac{1}{3}$.

The data scatter between these experiments and those of Dukowicz appears to be of the same order. The most uncertain measurement seems to be that of the electron and ion concentrations, and the nonuniformity in these quantities with space and time. It is felt that the majority of the scatter is caused by this effect.

The appropriate theoretical result for both the thin and thick sheath solutions[1,5,8] is shown on Fig. 7 and compared with average lines from the experimental results. The experiments reported here lie below the theory[6,7] at low values of S and closer to the theory at the higher values of S. There is some uncertainty in the location of the theoretical lines since the theories are based on conditions along the conical surface. At the lower Knudsen numbers, the conditions along the cone surface can be related to the conditions ahead of the probe by inviscid conical flow theory. The most important change across the shock is the increase in density and temperature. If the flow time around the probe is too short to allow the formation of additional ions, then the increase in ion density will be proportional to the increase in neutral density. For these Mach numbers and cone angles, the density increase is about 2. A proportional increase in neutral and ion densities has no effect on the S parameter but does decrease $J(\lambda_\phi/L)$ inversely as the square root of the density. The assumption of no formation of ions about the probe has been used in performing the theoretical predictions. While the condition of no ion formation is probably correct for the lower density conditions and smaller probes, the inviscid cone theory is not really applicable at the lower Reynolds number conditions. At higher densities, equilibrium ionization may occur across the shock which will lead to considerably greater increases in ion densities.

Of the three theoretical results shown in Fig. 7, the prediction based on the assumption of the sheath thin with respect to the boundary layer[5] seems to fit the data most closely and particularly so at low values of S. This agreement is probably fortuitous since the thin sheath assumptions are particularly inappropriate at low S. The slope of the present experimental data is greater than that predicted by any of the theories but closest to the value of 0.5 of the thin sheath result. The effect may be caused by an increase in ionization across the conical shock wave at lower Kn numbers, which also corresponds to higher S values in these experiments. This effect has not been considered in the theoretical predictions. Enough information is not available to properly assess this possibility. The thick sheath theories[1,8] agree fairly well with each other and do lie within the data band; however, they predict a slope with S considerably less than that indicated by the present experiments. The experiments of Dukowicz[7] are in better agreement with these theories over the lower range of S values,

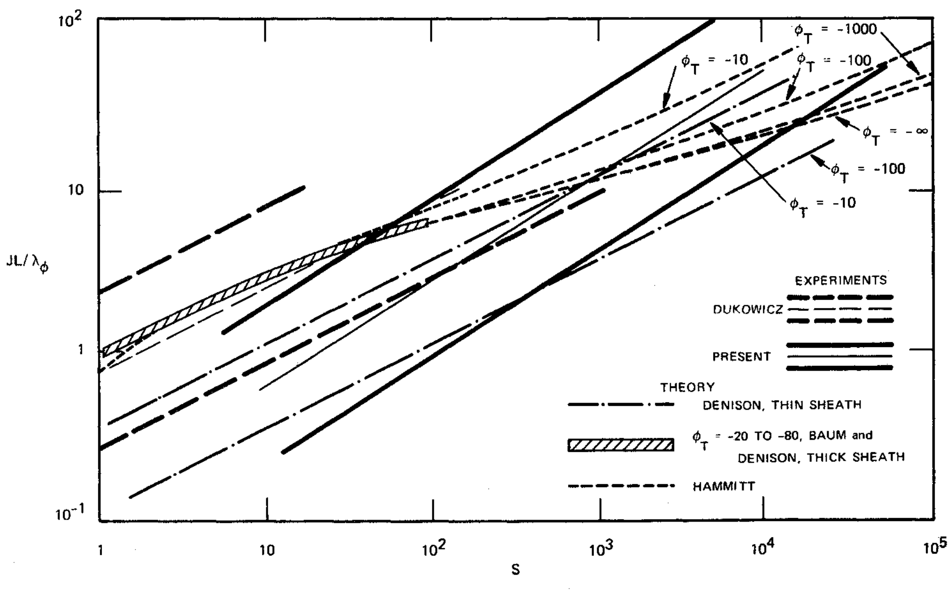

Fig. 7 Comparison of experimental results with theories.

and the slope of these data is closer to the theoretically predicted slope.

A comparison of the experiments with the theoretical predictions of DeBoer and Johnson[6] and Dukowicz[7] has not been made in Fig. 7. The DeBoer and Johnson[6] result is identical to that of Ref. 1 at $\phi_T = \infty$ and large values of S which is the range of applicability of DeBoer and Johnson's work. Dukowicz's[7] result is also essentially the same as the result of Ref. 1 at $\phi_T = \infty$, if λ_ϕ/L is small. A comparison of these theoretical results is shown in Fig. 8.

All the theories seem to be much more consistent with each other than with the experiments. The experiments cannot be used to evaluate the merits of the individual theories.

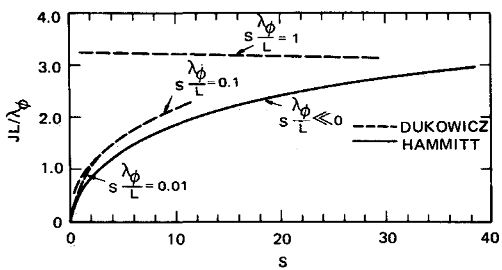

Fig. 8 Comparison of experimental results with theories.

Application of Data

A practical application of the conical electrostatic probe is to determine electron densities in a supersonic plasma stream. The experimental data presented here provide a means of doing so. If the straight line drawn through the average of the data on the log log plot is taken as a representation of that data, a simple empirical analytic relation can be written.

$$JL/\lambda_\phi = 0.135\, S^{2/3} \tag{5}$$

This relation is awkward to use to determine ion density since the ion density appears in both $J(\lambda_\phi/L)$ and S. The combination of these two parameters, which is independent of ion density, is

$$JS^{1/2}L/\lambda_\phi = (eI/\varepsilon_o u_\infty \pi \sin\theta)(eK/-2\phi_p u_\infty L)^{1/2} \tag{6}$$

The data correlation relation can be written in terms of this parameter to give either

$$JL/\lambda_\phi = 0.425[S(JL/\lambda_\phi)^2]^{2/7} \tag{7}$$

or

$$S = 5.5[S(JL/\lambda_\phi)^2]^{3/10} \tag{8}$$

where only terms on the left-hand side contain the ion density term.

References

[1] Hammitt, A. G., "Negatively Charged Electrostatic Probes in High Density Plasma," TRW Rept. 06488-6433-R0-00, June 1970, Redondo Beach, Calif.

[2] Jordan, E. C., "Electromagnetic Waves and Radiating Systems," Prentice-Hall, Englewood Cliffs, N.J., 1950, Chap. 9.

[3] Scharfman, W. E. and Bredfeldt, H. R., "Experimental Studies of Electrostatic Probes for the Reentry Measurements Program—Phase B," Final Report, Subcontract 601–603 under Contract DA 30-069-AMC-333(Y), SRI Project 6138, July 1967, Stanford Research Institute, Menlo Park, Calif.

[4] Scharfman, E. E. and Taylor, W. C., "Use of Ion Probes in Supersonic Plasma Flow," *AIAA Journal*, Vol. 8, No. 6, June 1970, pp. 1067–1072.

[5] Denison, M. R., "Analysis of Flush Electrostatic Probes for Reentry Measurements," Rept. 06488-6065-R0-00, Sept. 1967, TRW, Redondo Beach, Calif.

[6] DeBoer, P. C. T. and Johnson, R. A., "Theory of Flat-Plate Ion-Density Probe," *The Physics of Fluids*, Vol. II, 1968, p. 909.

[7] Dukowicz, J., "Theory of Convection-Conduction Dominated Electrostatic Probes: Numerical Solution of the Two-Dimensional Flat Plate Problem," Rept. RA-2641-Y-1, Jan. 1969, Cornell Aeronautical Lab., Buffalo, N. Y.

[8] Baum, E. and Denison, M. R., "A Thick Sheath Boundary Layer Model for Conical Electrostatic Probes in Continuum Flow," TRW Rept. 06488-6456-R0-00, Sept. 1970, Redondo Beach, Calif.

[9] Dukowicz, J., "Mobility of NO^+ Ions in Air," *AIAA Journal*, Vol. 8, No. 4, April 1970, pp. 827–829.